Engineering Fracture Mechanics 178 (2017) 433–444

Contents lists available at ScienceDirect

Engineering Fracture Mechanics

journal homepage: www.elsevier.com/locate/engfracmech

Estimation of fracture toughness and shear yield stress of orthotropic materials in cutting with rotating tools

Kazimierz A. Orlowski [a], Tomasz Ochrymiuk [b], Jakub Sandak [c,d,*], Anna Sandak [c]

[a] Gdansk University of Technology, Faculty of Mechanical Engineering, Department of Manufacturing Engineering and Automation, Narutowicza 11/12, Gdansk, Poland
[b] The Szewalski Institute of Fluid-Flow Machinery, Polish Academy of Sciences, Department of Transonic Flows and Numerical Methods, Fiszera 14, Gdansk, Poland
[c] IVALSA/CNR Trees and Timber Institute, via Biasi 75, San Michele all'Adige, TN, Italy
[d] University of Primorska, Faculty of Mathematics, Natural Sciences and Information Technology, Glagoljaška 8, 6000 Koper, Slovenia

ARTICLE INFO

Article history:
Received 9 May 2016
Received in revised form 17 January 2017
Accepted 24 February 2017
Available online 15 March 2017

Keywords:
Fracture toughness
Shear yield strength
Wood cutting
Cutting edge
Timber structure assessment

ABSTRACT

The cutting force is an energetic effect of splitting material, and might be considered from a point of view of modern fracture mechanics. Forecasting of the shear plane angle in cutting broaden possibilities for modelling of the cutting process even for thin uncut chips. Such mathematical model has been developed here for description of the orthotropic materials' cutting on the base of fracture theory, and includes work of separation (fracture toughness) in addition to the material plasticity and friction. The original methodology of simultaneous determination of the fracture toughness and the shear yield strength on the basis of wood cutting forces (or cutting power) is also presented in this paper. The set of data necessary for computation can be easily obtained while cutting wood with common rotating tools, such as a circular saw or a router bit. The results generated include both fracture toughness and shear yield stresses in the shear plane, separately for two anatomical directions of wood. The simplicity and reliability of this method provides wide range of practical applications.

1. Introduction

Estimation of the fracture toughness of materials is a challenging task, especially when accompanying with low yield stress. Wood may be described as an orthotropic material; having unique and independent mechanical properties in the directions of three mutually perpendicular axes: longitudinal (L), radial (R), and tangential (T). The longitudinal axis direction is parallel to the fibers course. The radial axis is normal to the growth rings, while the tangential axis is perpendicular to the grain but tangent to the growth rings. Elastic properties of wood are usually described by twelve material constants, where nine of these are independent [25]. Three Young's moduli E (moduli of elasticity), denoted by E_L, E_R, and E_T, that are corresponding to longitudinal, radial, and tangential axes of wood. Three moduli of rigidity (or shear) G, indicating the resistance to deflection of a member caused by the shear stresses, that are denoted by G_{LR}, G_{LT}, and G_{RT} and correspond to the elastic constants in the LR, LT, and RT planes respectively. Lastly, six Poisson's ratios ν_{LR}, ν_{RL}, ν_{LT}, ν_{TL}, ν_{RT}, and ν_{TR}, are used to characterize material, where the first letter of the subscript refers to the direction of applied stress and the second

* Corresponding author at: IVALSA/CNR Trees and Timber Institute, via Biasi 75, San Michele all'Adige, TN, Italy.
E-mail addresses: korlowsk@pg.gda.pl (K.A. Orlowski), tomasz.ochrymiuk@imp.gda.pl (T. Ochrymiuk), sandak@ivalsa.cnr.it (J. Sandak), anna.sandak@ivalsa.cnr.it (A. Sandak).

http://dx.doi.org/10.1016/j.engfracmech.2017.02.023
0013-7944/

Nomenclature

Φ_c	shear angle
$\Phi_{G\text{-}vc}$	an angle between grains and the cutting speed direction
α	confidence level
β_μ	friction angle
γ	the shear strain along the shear plane
γ_f	rake angle
$\overline{\varphi}$	an average angle of tooth contact with a workpiece
φ	angular tooth position
φ_1	entrance angle
φ_2	exit angle
ρ	density
μ	the coefficient of friction between wood and the rake face of the cutting edge
$\tau_{\gamma\perp}$	yield stress perpendicular to the fibers
$\tau_{\gamma\|\|}$	yield stress along the fibers direction
$\tau_{\gamma\|\|\perp}$	the shear yield stress for indirect cutting speed direction
a	position of the workpiece
a_1 and a_2	slope coefficients
b_1 and b_2	linear regression model intercepts
D	circular saw blade diameter
F_c^H	cutting force per tooth
f_z	feed per tooth
h	uncut chip thickness
H_p	workpiece height (depth of cut)
I	measured current
$I_{cutting}$	electrical current in cutting
$I_{iddling}$	electrical current in idling
I_{total}	total electrical current
L	length of cube
MC	wood moisture content
MOR	modulus of rupture
n_b	number of saw blades
$\overline{P}_{cw}$	cutting power
P_E	real electric power
P_{EM}	nominal electric power of the engine driving circular saw was
PF	power factor
Q_{shear}	the friction correction
r	Pearson's correlation coefficient
$R_\perp$	fracture toughness perpendicular to the fibers
$R_{\|\|}$	fracture toughness along the fibers
$R_{\|\|\perp}$	a fracture toughness for indirect (neither || nor $\perp$) position of cutting speed
S_t	overall set (or cutting width)
U	electrical tension
v_c	cutting speed
W	width of cube
w_1 and w_2	widths of cutting edges
Z	material dependent parameter
z	number of carbide tipped teeth
z_a	an average number of teeth being in the contact with the kerf

letter to the direction of lateral deformation. Several other mechanical/strength properties are frequently considered beside above material constants during structure design [25]. Among these fracture toughness, which is also called as the specific work of fracture R is especially important as directly affects a critical value of the stress intensity factor Kc [22]. The latter is considered as a property indicating resistance of material to cracking [4]. The linear fracture mechanics is usually used for its assessment, assisted by a number of semi-destructive methods. Indentations tests are for instance based on the correlation between hardness and fracture toughness of material, in some cases including these of biological origin. Such indentation test can be either dynamic or quasi static, and may be performed at the micro or macro level [26]. Likewise, scratch-cutting test bases on the correlation between fracture toughness and materials' resistance to scratch. Pull-out tests are frequently used to estimate interfacial fracture toughness in fibrous materials. However, this test is not suitable for all materials

(wood for example) due to not proper appearance of fracture surfaces required for pull-out [2]. Wedge splitting tests [48] allows the estimation of wood fracture toughness. The energy release rate required to initiate and propagate the crack can be measured during stable crack growth experiment [3]. Optical methods were used for determination of the mechanical stresses distribution as well as shear angle determination while cutting wood in different anatomical directions [33]. The orthotropic theory allows estimation of the fracture toughness by visual analysing of displacement fields at the near-tip zone assisted with digital image correlation [46,50].

Several scientific studies, both theoretical and experimental, were dedicated to understand cutting forces involved in material cutting by linking this process to the modern fracture mechanics [6,4,10,20,53]. Accordingly, analysis of the cutting forces may be an alternative approach for determination of fracture toughness and shear yield stresses. It has been applied for various materials and cutting configurations [7,42,43,38,41,51,52,9,29]. Cutting of orthotropic bio-materials is particularly complex process influenced by many parameters; microstructure, morphology, mechanical properties of material, loading mode, velocity of deformation, moisture, temperature, not to mention cutting edge geometry and machine/process conditions. Numerical models of cutting forces involved in wood cutting by considering elements of fracture mechanics were developed by Laternser et al. [28] and followed by Merhar and Bučar [32] as well as Orlowski et al. [36]. An important limitation is a narrow set of reliable reference raw material data, such as values of wood fracture toughness and shear yield strength varying in a function of the grain angle, to be possibly used for validation of models [49].

The relationship between cutting forces and uncut chip thickness, in case of cutting most materials, is considered as linear [4]. The only exception is a zone of extremely thin chips when cutting mechanisms differs noticeably. The same relation was reported by Csanády and Magoss [14] for wood and wood-based materials. It was experimentally confirmed by authors during several cutting tests on the frame sawing machine [35,38,41] as well as on the circular sawing machine [21]. Hence, it is possible to accurately describe the cutting force versus uncut chip thickness relation by means of two experimental points resulting of at least two independent measurements.

The goal of this work was to develop an alternative methodology and measurement routine for simultaneous determination of wood fracture toughness and shear yield strength on the basis of cutting tests performed with rotating tools on standard woodworking machinery.

1.1. Cutting of orthotropic materials with rotating tool

The first systematic studies of cutting forces with different grain orientations and the study of the different chip types and formation started in the 1950s and 1960s with the work of Kivimaa [23], Franz [16], McKenzie [31], being recently re-examined by Wyeth et al. [54]. Cutting speed directions in case of cutting along fibers, perpendicular (across) to the fibers, and for indirect cutting direction are shown in Fig. 1. Cutting forces for orthotropic materials are commonly calculated on the basis of the specific cutting resistance k_c (cutting force per unit area of cut), which is in the case of wood cutting the function of the following factors: wood species, cutting direction angle (cutting edge position in relation to wood grains), moisture content, wood temperature, tooth geometry, tooth dullness, chip thickness, among others [47,1,34,44]. Values of cutting resistance for pine wood, considering the position of the cutting edge in relation to the grains (fibers) is a common reference for estimation of k_c for other wood species. For the latter, the cutting resistance of pine wood is multiplied by specific factors empirically determined for each species. It has to be mentioned that the specific cutting resistance differs accordingly to the cutting operation and/or process kinematics. The specific cutting resistance may be calculated for indirect positions of the cutting speed direction from formulae developed in the field of material strength, by considering the $\Phi_{G\text{-}vc}$ angle [34]. The transformation equation for the plane stress was applied here according to Gere [17].

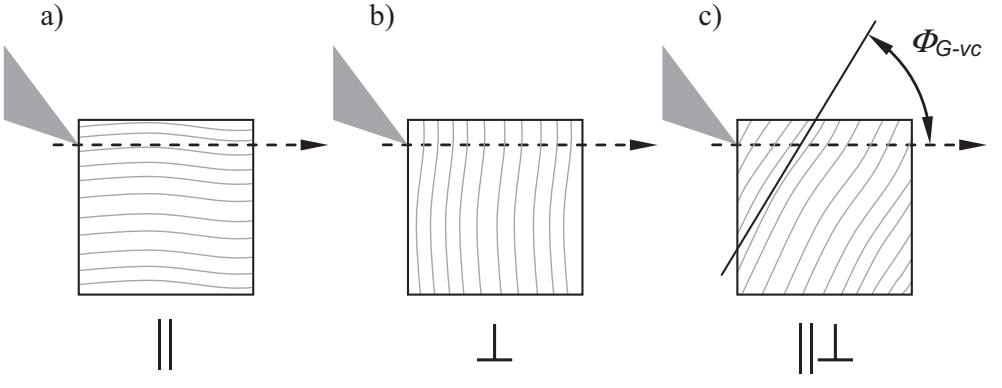

Fig. 1. Cutting speed directions when splitting orthotropic materials; axial || cutting along fibers (a), perpendicular ⊥ cutting across fibers (b) and indirect || ⊥ direction (c).

The kinematics of cutting with rotating tool is schematically presented in Fig. 2 as an example of sawing with a circular saw. The cutting speed direction v_c changes its position relatively to the wood fiber direction along the tool path. Values of entrance angle φ_1 and exit angle φ_2 depends on the cutting geometry and can be computed according to Eqs. (1) and (2) repectively.

$$\varphi_1 = \arccos\frac{2(H_p + a)}{D} \tag{1}$$

$$\varphi_2 = \arccos\frac{2a}{D} \tag{2}$$

An average value of uncut chip thickness $\overline{h}$ should be taken into account instead of feed per tooth f_z in case of cutting with circular saw blades [36]. Hence, the cutting power P_{cw} may be expressed by means of certain material constants and cutting process variables as in Eq. (3). This formula was developed originally for isotropic materials by Atkins [6], and later adapted for the case of wood sawing by Orlowski and Atkins [38], and Orlowski et al. [36]:

$$\overline{P}_{cw} = z_a \cdot \frac{\tau_{\gamma\|\perp} S_t \gamma}{Q_{shear}} v_c \overline{h} + z_a \cdot \frac{R_{\|\perp} S_t}{Q_{shear}} v_c \tag{3}$$

where $\overline{h}$ – an average value of uncut chip thickness (Eq. (4)), z_a – an average number of teeth being in the contact with the kerf (Eq. (6)), γ – the shear strain along the shear plane (Eq. (7)), Q_{shear} – the friction correction (Eq. (9)), S_t – overall set (or cutting width, considered also as a kerf in the case of circular sawing), $R_{\|\perp}$ – a fracture toughness for indirect (neither || nor $\perp$) position of cutting speed corresponding to an average angle $\overline{\varphi}$, $\tau_{\gamma\|\perp}$ – the shear yield stress along the shear plane for indirect cutting speed direction, corresponding also to an average angle $\overline{\varphi}$.

$$\overline{h} = f_z \sin\overline{\varphi} \tag{4}$$

where f_z – feed per tooth, and $\overline{\varphi}$– an average angle of teeth contact with a workpiece (Eq. (5))

$$\overline{\varphi} = \frac{\varphi_1 + \varphi_2}{2} \tag{5}$$

$$z_a = \left(\frac{\varphi_2 - \varphi_1}{\frac{360^\circ}{z}}\right) \tag{6}$$

where z – number of teeth in the sawblade.

The shear strain γ along the shear plane could be calculated as in Eq. (7) [6,12]:

$$\gamma = \frac{\cos\gamma_f}{\cos(\Phi_c - \gamma_f)\sin\Phi_c} \tag{7}$$

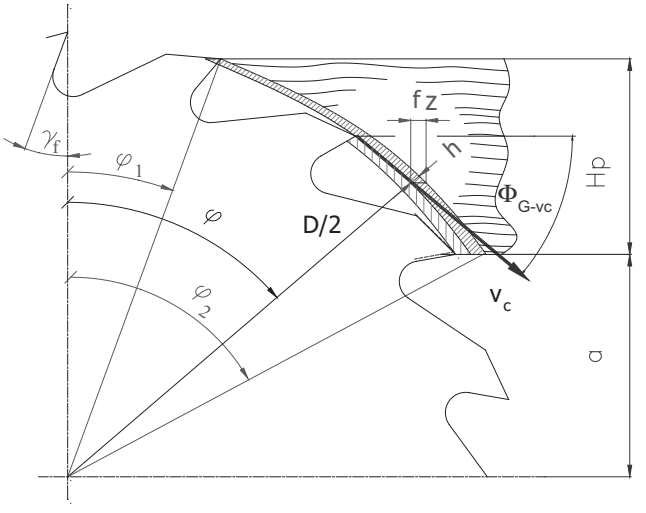

Fig. 2. Sawing kinematics on circular sawing machine: f_z – feed per tooth, D – circular saw blade diameter, h – uncut chip thickness, H_p – workpiece height (depth of cut), a – position of the workpiece, φ – angular tooth position, φ_1 – entrance angle, φ_2 – exit angle, $\Phi_{G\text{-}vc}$ – an angle between grains and the cutting speed direction, γ_f – rake angle.

where Φ_c is the shear angle which defines the orientation of the shear plane with respect to cut surface (Eq. (8)). The shear angle for higher values of uncut chip thicknesses or feed per tooth f_z (h) can be calculated with the Merchant equation (because for those uncut chip values $\Phi_c = const.$ [12]). Though, in other cases an equation proposed by Atkins [6] should be applied:

$$\Phi_c = (\pi/4) - (1/2)(\beta_\mu - \gamma_f) \tag{8}$$

The friction correction Q_{shear} is determined according to Atkins [6] as:

$$Q_{shear} = [1 - (\sin\beta_\mu \sin\Phi_c / \cos(\beta_\mu - \gamma_f)\cos(\Phi_c - \gamma_f))] \tag{9}$$

where β_μ – friction angle (Eq. (10)), the friction correction $Q_{shear} = 1$ when $h = 0$.

$$\beta_\mu = \tan^{-1}\mu \tag{10}$$

where μ – the coefficient of friction between wood and the rake face of the cutting edge.

As a matter of fact, the shear angle Φ_c is not the Merchant value and therefore should be corrected according to the ratio of R and τ_γ [48,6]. It was found that shear angle Φ_c values as computed according to Eq. (8) are frequently slightly higher than those measured experimentally. Unfortunately, very limited reference material-dependent data for wood cutting was reported so far, except for results of pine sawing [8,13]. It is important to mention that the model (Eq. (3)) assumes perfect sharpness of the cutting edge. Moreover, both ploughing effect [51,11] and chip momentum are disregarded [36] due to moderate values of feed speeds while sawing wood.

2. Algorithm for the determination of material mechanical properties in cutting

The method for the wood fracture toughness and shear strength determination presented here is based on the cutting theory originally proposed by Atkins and Vincent [5]. Its practical implementation toward orthotropic materials (such as wood) in various configurations and in a range of ordinary machining processes was reported by authors [37]. It was demonstrated that the fracture toughness $R_{\parallel\perp}$ and the shear yield stress $\tau_{\gamma\parallel\perp}$ for indirect/intermediate directions (regarding wood fibers) may be computed on the basis of $R_\perp$ and $\tau_{\gamma\perp}$ [36]. In that case, both $R_\perp$ and $\tau_{\gamma\perp}$ were empirically determined in the cross cutting experiment described in [41]. However, values of the fracture toughness $R_\parallel$ and the shear yield stress $\tau_{\gamma\parallel}$ for the longitudinal direction were calculated adopting corresponding coefficients reported in literature. Recently, Kopecký et al. [24] developed an alternative methodology for determining $\tau_{\gamma\parallel\perp}$ and $R_{\parallel\perp}$ within orthotropic materials by means of circular sawing. Though, both values are appropriate only for selected directions, related to the average angle of tooth contact with a workpiece $\overline{\varphi}$ and may not be therefore considered as material constants.

Hlaskova et al. [21] proposed a combined method to determine toughness and strength parameters for the tooth cutting edge principal positions for longitudinal and perpendicular cutting speed directions. Nevertheless, in this method two types of machine tools of different sawing kinematics must be applied, and it seems to be a main disadvantage of the method. A different way to estimate the fracture toughness and yield stress of wood along || and across ⊥ fibers was reported by Orlowski et al. [37]. In that case, at least four cutting tests have to be conducted with a rotating tool i.e. a circular saw blade. It is important to assure minimum two diverse levels of feed speed v_f and at least two varying chip thicknesses $\overline{h}$, corresponding to varying cutting depths H_p. In general, increased number of feed speed levels and/or cutting depths results in the improvement of the measurement reliability and reducing estimation error. A set of linear equations (at least two) for cutting force per tooth F_c^H in sawing workpiece of thickness H is determined on the basis of experimental results:

$$\begin{cases} F_{c1}^{H_1} = a_1\overline{h} + b_1 \\ F_{c2}^{H_2} = a_2\overline{h} + b_2 \end{cases} \tag{11}$$

Eq. (11) corresponds to Eq. (3), but divided by z_a and v_c. It was proven by Orlowski and Pałubicki [41] that it is possible to determine values of the shear yield stress $\tau_{\gamma\perp\parallel 1}(H_1)$ and $\tau_{\gamma\perp\parallel 2}(H_2)$ on the base of Eq. (11), as slopes a_1 and a_2, can be also expressed as in Eqs. (12) and (13) respectively:

$$a_1 = \frac{\tau_{\gamma\perp\parallel 1} w_1 \gamma_1}{Q_{shear1}} \tag{12}$$

and

$$a_2 = \frac{\tau_{\gamma\perp\parallel 2} w_2 \gamma_2}{Q_{shear2}} \tag{13}$$

where w_1 and w_2 are widths of cutting edges, corresponding to the kerf S_t.

The shear strains along the shear plane γ_1 and γ_2, the shear angle Φ_c as well as the friction corrections Q_{shear1} and Q_{shear2} may be, especially for higher values of h, calculated according to Eqs. (7)–(9) respectively. It is important to emphasise that all above parameters are calculated independently for each equation from the system (11).

Accordingly, the specific work of surface separation/formation (fracture toughness) $R_{\perp\|1}$ and $R_{\perp\|2}$ can be calculated from the intercept values b_1 and b_2 for cutting depths H_1 and H_2:

$$b_1 = \frac{R_{\perp\|1} w_1}{Q_{shear1}} \tag{14}$$

and

$$b_2 = \frac{R_{\perp\|2} w_2}{Q_{shear2}} \tag{15}$$

Values of the stress $\tau_{\gamma\perp\|1}$ and $\tau_{\gamma\perp\|2}$ as well as of the fracture toughness $R_{\perp\|1}$ and $R_{\perp\|2}$ as derived from Eqs. (11)–(15), are intermediary; neither parallel nor perpendicular to the woody grain direction. Consequently, it is necessary to extract the explicit values for each of the above specific material characteristics. Orlicz [34] applied the plane stress transformation equation for determination of specific cutting resistance in indirect positions of the cutting speed direction. The same method is commonly used in general mechanics of materials to transform the stress components from one set of axes to another [17]. Such approach is of a great advantage for analysis of orthotropic materials, such as wood. Currently, Orlowski et al. [36,37] and Hlaskova et al. [21] implemented plane stress transformation equation in different cutting speed position for computation of the shear yield stress and fracture toughness as tensor values. Hence, the following set of equations (Eqs. (16) and (17)) provide a mathematical base for that, by considering an effect of the angle between the wood grain and the cutting speed direction $\Phi_{G\text{-}vc}$. As the shearing take place in the shear plane, the value of the shear angle Φ_c is considered in the system of Eq. (16):

$$\begin{cases} \tau_{\gamma\perp\|1} = \tau_{\gamma\|}\cos^2(\Phi_{G-vc1} + \Phi_c) + \tau_{\gamma\perp}\sin^2(\Phi_{G-vc1} + \Phi_c) \\ \tau_{\gamma\perp\|2} = \tau_{\gamma\|}\cos^2(\Phi_{G-vc2} + \Phi_c) + \tau_{\gamma\perp}\sin^2(\Phi_{G-vc2} + \Phi_c) \end{cases} \tag{16}$$

$$\begin{cases} R_{\perp\|1} = R_{\|}\cos^2\Phi_{G-vc1} + R_{\perp}\sin^2\Phi_{G-vc1} \\ R_{\perp\|2} = R_{\|}\cos^2\Phi_{G-vc2} + R_{\perp}\sin^2\Phi_{G-vc2} \end{cases} \tag{17}$$

where $\tau_{\gamma\|}$ – yield stress along the fibers direction, $\tau_{\gamma\perp}$ – yield stress perpendicular to the fibers, $R_{\|}$ – fracture toughness along the fibers, and $R_{\perp}$ – fracture toughness perpendicular to the fibers.

It was demonstrated that Tsai-Hill failure theory may be alternatively used to determine the shear yield stresses in orthotropic materials [30]. However, that approach may be implemented in the quasi-static off-axis tension test and is problematic for implementing dynamic effects of the material cutting.

According to the theory of the wood machining, the favourable chip formation for rake angle $\gamma_f > 35°$ results in the off-cut formation by bending [16,45,4,14]. Furthermore, Atkins [4] stated that only for a constant uncut chip thickness offcut can be formed in elastic bending, when the fracture toughness parallel to the surface is smaller than in other directions, i.e. in anisotropic materials. The cutting conditions applied justify therefore the numerical approach chosen (Eqs. (16) and (17)) as the rake angle of tools selected for our tests was $\gamma_f = 25°$.

3. Computational example: circular saw case

The novel method for determination of mechanical properties of orthotropic materials by means of the dedicated cutting test was adopted for a case of the circular sawing process. The following is a brief description of the performed experiment and demonstration of the new measurement routine.

3.1. Materials

Scots pine (*Pinus sylvestris* L.) wood originated from the Forest Inspectorate Lipusz in the Baltic Natural Forest Region (Poland) was used for preparation of experimental materials. Samples were in the shape of cubes of width $W = 50$ mm and length $L = 2200$ mm, with two heights of $H_1 = 50$ mm and $H_2 = 100$ mm. The wood moisture content was $MC = 35\%$ and density $\rho = 510$ kg m^{-3}. The processed timber temperature was corresponding to the room conditions and was 20 °C.

The reference material characteristics were measured in an independent experiment with pine wood ($\rho = 520$ kg m^{-3}). The values for perpendicular direction of cutting were determined according to the methodology described by Orlowski and Pałubicki [41], while for parallel direction were estimated on the basis of data adopted from the literature [36]:

- fracture toughness; $R_{\perp} = 1.30$ kJ m^{-2} (cutting tests) and $R_{\|} = 0.065$ kJ m^{-2} (estimated as a reference from the paper by Aydin et al. [8]),
- shear yield stress; $\tau_{\gamma\perp} = 20.9$ MPa (cutting tests) and $\tau_{\gamma\|} = 5.2$ MPa (computed as $\tau_{\gamma\|} = 0.125 \cdot MOR$, where $MOR = 41.6$ MPa – modulus of rupture referred as a bending strength, value taken from Krzosek [27]).

The value of friction coefficient $\mu = 0.9$ for pine wood was chosen according to Glass and Zelinka [18].

3.2. Tool and machine

The cutting tests were carried out on the one shaft multi rip sawing machine PWR301 (TOS Svitavy, Czech Republic) at the Complex sawmill in Dziemiany (Baltic Natural Forest Region, Poland). The nominal electric power of the motor driving circular saw was P_{EM} = 45 kW. The cutting kinematics was up-sawing, number of saw blades n_b = 1, clearance of a circular saw blade over the workpiece 5 mm and feed speed v_f applied at three levels: 10, 20 and 40 m min^{-1}. Different tools and cutting conditions were used for sawing samples of different thicknesses:

- H_p = 100 mm: cutting speed v_c = 69.6 m s^{-1} (3800 rpm), the circular saw used was produced by Aspitech (Poland), external diameter D = 350 mm, collar diameter d = 80 mm saw blade thickness s = 2.5 mm, overall set S_t = 3.9 mm, number of carbide tipped teeth z = 18, and side rake angle γ_f = 25°,
- H_p = 50 mm: cutting speed v_c = 69.9 m s^{-1} (4450 rpm), the circular saw used was produced by Aspitech (Poland), external diameter D = 300 mm, collar diameter d = 80 mm saw blade thickness s = 2.5 mm, overall set S_t = 3.2 mm, number of carbide tipped teeth z = 18, and side rake angle γ_f = 25°.

3.3. Cutting force measurements

Electrical power consumption of the sawing machine was measured by using AC/DC current transducer DHR 100C10 (LEM USA Inc., USA), 8-channel isolation amplifier NI SCXI1125 (National Instruments, USA), 4-Slot Chassis NISCXI 1000DC (National Instruments, USA) and PC computer with the NI PCI 6281 A/D conversion board (National Instruments, USA). The current transducer was installed on the single-phase power cable connected to the three-phase electrical motor; however, it was assumed that the corresponding values of current were identical in all electric phases [40]. Sampling frequency was 1000 Hz with a signal resolution of 18 bits. The sampling rate and accuracy of the experimental hardware allowed precise measurement of even minor changes in the electrical current due to wood processing. The real electric power P_E was calculated as in Eq. (18):

$$P_E = \sqrt{3}\cdot U \cdot I \cdot PF \tag{18}$$

where U – electrical voltage (U = const. = 400 V_{AC}), I – measured current (in A), PF – power factor ($PF = \cos\Phi$).

The power factor PF = 1 for purely resistive load, what is not a case of electrical motors where induction-related loads varies depending on the working conditions. It was determined empirically that PF = 0.3 for idling, PF = 0.8 for cutting samples H_2 = 100 mm, and PF = 0.55 for cutting samples H_1 = 50 mm. A relation between PF and feed speed was assumed as linear in the whole range of the used cutting conditions. An example of raw results (electrical current) registered while sawing experimental samples is presented in Fig. 3. It is clear that each cutting cycle differed from the idling run of the machine. The quantity of the electrical energy consumed for idle running of the machine ($I_{iddling}$) was extracted from the total power (I_{total}) in order to quantify energy used for pure cutting ($I_{cutting}$). Subsequently, the average cutting power ($\overline{P}_c$) and the mean value of the cutting force ($\overline{F}_c$) per tooth were determined.

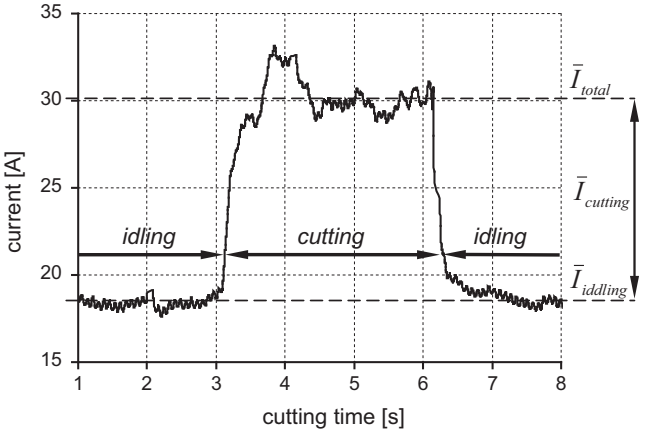

Fig. 3. Registered electrical current (one phase) variations during the cutting experiment with circular saw (pine wood (*Pinus sylvestris* L.) H_2 = 100 mm, feed speed v_f = 40 m min^{-1}).

4. Implementation of the algorithm

Series of cutting experiments were performed on the circular sawing machine in order to acquire the set of data required for determination of the material characteristics. The schematic of the experiment configuration is presented in Fig. 4.

All the resulting cutting forces were linearly regressed in a function of the uncut chip thickness. Statistical analyses of the regressions were made at the confidence level $\alpha = 0.05$. The set of experimental quantities obtained for varying feed speeds and cutting depths were plotted in the single chart, as presented in Fig. 5. The linear regression models were developed in each case and these qualities were characterized by the Pearson's correlation coefficient. The values corresponding to models presented in Fig. 5 were $r = 0.93$ and $r = 0.99$ for H_1 and H_2 thicknesses respectively.The average angle of the tooth contact with a workpiece was computed according to Eq. (5), and assuming cutting of sample $H_1 = 50$ mm was $\overline{\varphi}_1 = 32.8^\circ$, while $\overline{\varphi}_2 = 40.1^\circ$ for sample of $H_2 = 100$ mm. Correspondingly, the average cutting force per tooth $\overline{F}_c$ for a specific cutting direction regarding grain course $\overline{\varphi}$ can be expressed as on Eqs. (19) and (20) for the samples of thickness $H_1 = 50$ mm and $H_2 = 100$ mm respectively.

$$\overline{F}_c^1(\overline{\varphi}_1 = 32.8^\circ) = 139644\overline{h} + 1.25 \tag{19}$$

$$\overline{F}_c^2(\overline{\varphi}_2 = 40.1^\circ) = 179580\overline{h} + 2.12 \tag{20}$$

The extent of the measurement repeatability was quantified as a maximum standard deviation SD, computed independently for the slope ($SD_a = 4024$ N m^{-1}) and intercept ($SD_b = 0.64$ N) of the linear fit. A set of material characteristics can be extracted from the above equations by following the method of Atkins [4], namely; values of the slope coefficients $a_1 = 139644$ N m^{-1} and $a_2 = 179580$ N m^{-1} as defined in Eqs. (11)–(13).The orientation of shear plane with regard to cut surface $\Phi_c = 36.51^\circ$ was computed on the base of Eq. (8), for $\mu = 0.9$ and $\beta_\mu = 41.98$. At the same time, the shear strain along the shear plane $\gamma = 1.59$ and the friction correction $Q = 0.575$ were computed according to Eqs. (7) and (9). Finally, it was possible to determine the shear yield stresses for two indirect cutting directions: $\overline{\varphi}$; $\tau_{\gamma||\perp}(32.8^\circ) = 15.78$ MPa, and $\tau_{\gamma||\perp}(40.1^\circ) = 16.65$ MPa. The toughness R was determined from the linear regression model intercepts $b_1 = 1.25$ and $b_2 = 2.12$ (Eq. (11)) and converted into values specific for two intermediate angles $\overline{\varphi}_1$ and $\overline{\varphi}_2$ by means of Eqs. (14) and (15). The obtained values of fracture toughness are therefore $R_{||\perp}(32.8^\circ) = 390.6$ J m^{-2}, and $R_{||\perp}(40.1^\circ) = 543.6$ J m^{-2}.

The system of Eq. (17) is resolved in order to determine the shear yield stresses τ_γ for two principal anatomical directions of wood; along to the fibers (grain) $\tau_{\gamma||} = 5.09$ MPa and perpendicular $\tau_{\gamma\perp} = 17.31$ MPa. The comparison of the obtained $\tau_{\gamma\perp}$ with corresponding values from reference experiments (20.9 MPa) revealed that the second are slightly larger (~3.59 MPa), as shown in Table 1. Correspondingly, the ratio $\tau_{\gamma||}/\tau_{\gamma\perp}$ determined experimentally was equal to 0.29, while $\tau_{\gamma||}/\tau_{\gamma\perp} = 0.24$ in case of the reference material characteristics. It has to be mentioned, however, that the reference value of $\tau_{\gamma||}$ was determined on the basis of modulus of rupture (MOR) obtained in the static bending tests [27]. The higher value of the $\tau_{\gamma||}/\tau_{\gamma\perp}$ ratio could be also related to the methodological approach applied as well as to different provenances of the materials [13]. It was reported by Green [19] that the wood shear strength parallel to the grain ranges from 3 to 15 MPa at 12% moisture content (MC). In another research by Kretschmann [25] the shear strength parallel to the grain for pine was estimated as 6.1 to 11.6 MPa at MC = 12%, while it was between 4.7 and 7.2 MPa in a case of wet pine wood. Slightly lower value of $\tau_{\gamma||}$ as assessed in this experiment may be therefore related to the effect of higher moisture content of machined wood (MC = 35%). Moreover, by following Green [19] the shear strength perpendicular to the grain was 2.5–3 times higher than the shear parallel to the grain. The same ratio obtained experimentally in this work was $\tau_{\gamma\perp}/\tau_{\gamma||} = 3.44$.

Wang et al. [51] and Blackman et al. [11] reported that values of the yield stress on the shear plane τ_γ estimated by means of cutting are relatively higher. It could be especially noticeable when characterize composite materials, such as wood. Wood is a complex composite of three natural polymers: lignin, cellulose and hemicellulose. All of these possess dissimilar

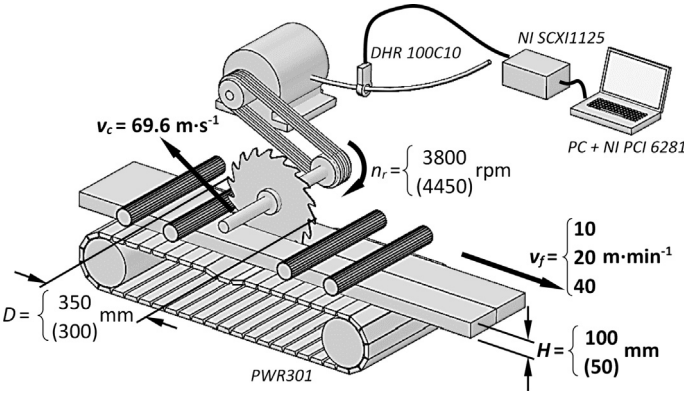

Fig. 4. Summary of the experimental design for estimation of fracture toughness and shear yield stress in cutting with circular saw.

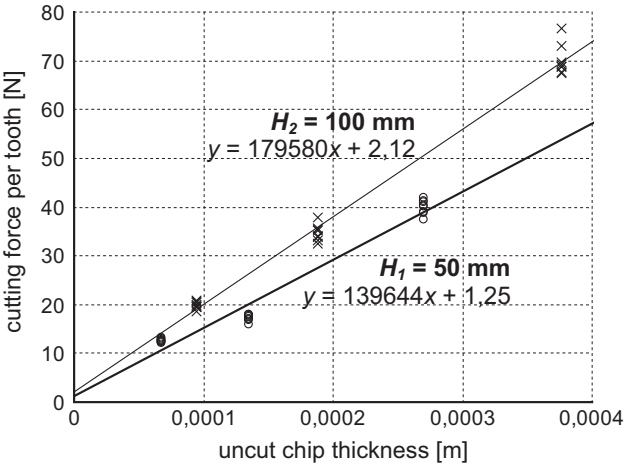

Fig. 5. Linear regression models for cutting force per tooth versus uncut chip thickness when sawing pine wood (*Pinus sylvestris* L.) of 50 mm and 100 mm thickness with varying feed speeds.

Table 1
Shear yield stress and fracture toughness of Scotch pine determined in cutting tests and static bending tests [8,27].

	Cutting test	Cutting test and static bending estimation
Shear yield stress along the grain $\tau_{\gamma\|\|}$ (MPa)	5.09	5.2
Shear yield stress perpendicular to the grain $\tau_{\gamma\perp}$ (MPa)	17.31	20.9[a]
Ratio $\tau_{\gamma\|\|}/\tau_{\gamma\perp}$	0.29	0.24
Fracture toughness along the grain direction $R_{\|\|}$ (J m^{-2})	22.2	65.0
Fracture toughness perpendicular to the grain direction $R_\perp$ (J m^{-2})	1286.7	1300.0
Ratio $R_{\|\|}/R_\perp$	0.017	0.05
Density ρ (kg m^{-3})	510	520
Moisture content *MC* (%)	35	12
Provenance	Lipusz	Leśny Dwór

[a] Values determined in cutting tests.

mechanical properties, each affecting the physics of cutting in a different way. The action of the cutting edge in the sawing process crashes and compacts anatomical components of woody tissues. Hence, in some cases it may lead to increase of the yield stress values. The similar phenomenon was also observed by different researchers while cutting other materials, including metals or plastics.

Predictions of the crack trajectories while cutting is a difficult task [4]. Particularly, during wood machining several physical processes occur simultaneously, such as deformation of the material ahead and below the tool, as well as fracturing in front of it in the opening (mode I) or shear (mode II) modes. Nevertheless, during separation processes of wood in cutting, deformation and fracturing take place not only in the crack opening mode (mode I), but also in sliding modes (for instance mode II – in-plane shear and mode III – antiplane shear) [49]. The explicit definition of the phenomena in the cutting zone is particularly problematic since the sawing process with circular saw blades is accompanied by high cutting speeds, cutting in the narrow slot, and continuously varying position of the cutting edge in relation to the wood grains. It is expected that recent technical developments in the field of high speed photogrammetry may allow detailed observations of the cutting zone during chip formations [15].

The system of Eq. (18) was also resolved in order to determine the specific work of the surface separation/formation (fracture toughness) R for two principal anatomical directions of wood; along the grain $R_{\|\|} = 22.2$ J m^{-2} and perpendicular $R_\perp = 1286.7$ J m^{-2}. The comparison of R values obtained with cutting and static bending tests revealed that $R_\perp$ are comparable for both methods, even if the ratio of $R_{\|\|}/R_\perp$ was slightly higher in the cutting test. Again, the latter values were determined with a compound methodology (cutting tests and static bending experiments) and adopted for the needs of this research from the literature. The other significant factor affecting differences noticed in experimental results are related to dissimilarities of wood sample provenances and physical properties. It has to be emphasised that there are very limited references reported for fracture properties of pine wood. Some available results from the corresponding research on Turkish pine were published by Aydin et al. [8] whereas the ratio $R_{\|\|}/R_\perp$ was 0.004.

The shear plane angle Φ_c changes according to the cutting conditions and especially in relation to the uncut chip thickness h. It is possible to predict Φ_c assuming its material dependency, as reported by Atkins [6] and Orlowski et al. [36,37]. In that case, the relationship for Φ_c prediction can be expressed as in Eq. (21) [6]:

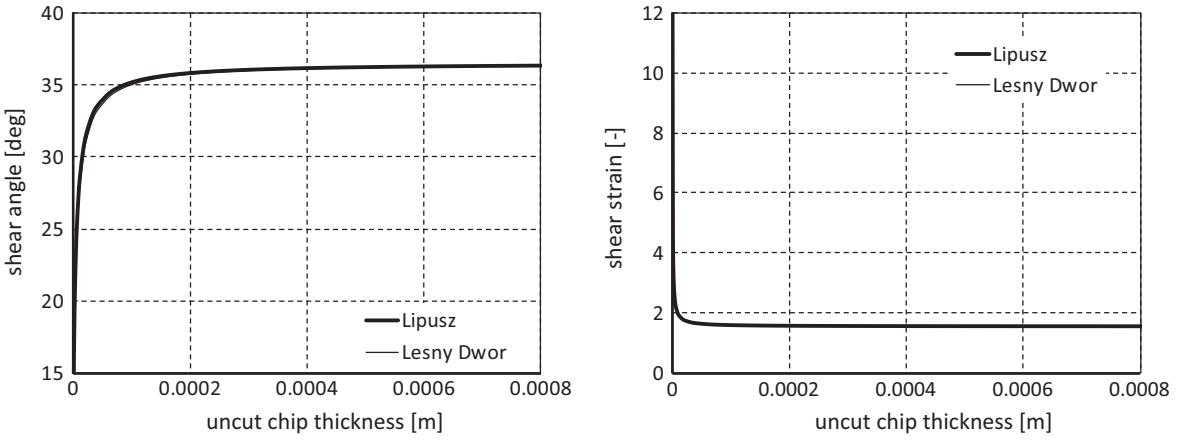

Fig. 6. Numerical models simulating an effect of the uncut chip thickness h on the shear plane angle Φ_c and shear strain γ *for* pine wood (*Pinus sylvestris* L.) samples of two provenances.

$$\left[1-\frac{\sin\beta_\mu\sin\Phi_c}{\cos(\beta_\mu-\gamma_f)\cdot\cos(\Phi_c-\gamma_f)}\right]\cdot\left[\frac{1}{\cos^2(\Phi_c-\gamma_f)}-\frac{1}{\sin^2\Phi_c}\right]$$
$$=-[\cot\Phi_c+\tan(\Phi_c-\gamma_f)+Z]\cdot\left[\frac{\sin\beta_\mu}{\cos(\beta_\mu-\gamma_f)}\left\{\frac{\cos\Phi_c}{\cos(\Phi_c-\gamma_f)}+\frac{\sin\Phi_c\sin(\Phi_c-\gamma_f)}{\cos^2(\Phi_c-\gamma_f)}\right\}\right] \tag{21}$$

where Z – is a parameter, which makes Φ_c material dependent, being computed as in Eq. (22):

$$Z=\frac{R}{\tau_\gamma\cdot\overline{h}} \tag{22}$$

A resulting model values of the shear plane angle Φ_c in relation to the uncut chip thickness in the case of sawing pine wood of H_1 = 100 mm were determined according to Eq. (21) and are shown in Fig. 6a. There are noticed significant changes to the Φ_c for very low average chip thicknesses. The value of the shear plane angle Φ_c becomes constant for h > 0.0003 m. Such changes at small depths of cut are the causes for the dramatic increase of the specific cutting pressure for small values of the feed per tooth, so-called 'size effect' as reported by Atkins [6], Atkins [4] and Orlowski et al. [39]. The obtained values of Φ_c for the thick uncut chips overlap each other even for samples of different examined provenances; Φ_c = 36.26° for wood originated from Lipusz and for wood from Leśny Dwór. On the contrary, the Merchant's equation (Eq. (8)) does not take into account raw material properties (as well as provenance) and therefore the value of shear plane angle Φ_c = 36.51° was slightly higher.

A similar model for prediction of the shear strain γ for varying uncut chip thickness was prepared on the base of Eq. (7) and is presented in Fig. 6b. It is evident that the value of γ changes dramatically for very small chips (h < 0.0001 m). However, the differences in the shear strain due to provenance (and related material properties) are insignificant, being in case of both provenances γ = 1.56.

The action of the cutting edge in the sawing process crash and compact anatomical components of woody tissue. It may lead to increase of the yield stress values, as was observed in our experiments. It can be related to the similar phenomenon in cutting metals as described by Atkins [4].

5. Conclusions

The novel method proposed here provides a unique possibility of simultaneous determination of various mechanical properties of orthotropic materials, including wood. It combines experimental cuttings for determination of reference values and modern fracture mechanics theory for the parameters extraction. Even though the circular sawing process is not a simple process of orthogonal cutting, it was proven to be suitable for accurately determine fracture toughness and shear yield strength for two principal directions regarding wood grains.

The results of the demonstration tests revealed that for pine wood originated from Poland, the ratio $R_{||}/R_{\perp}$ = 0.017 and $\tau_{\gamma||}/\tau_{\gamma\perp}$ = 0.29. Both values are slightly different than these reported in literature, but it can be explained by the methodological differences in the determination methods.

It was demonstrated that the sawing process with circular saw blades might become an alternative approach for determining the fracture toughness and shear yield strength of a wide variety of sawn timber. The possible application fields include on-line quality control of construction timber, but also assessment of material properties in existing structures. In

any case only small amount of material is removed during cutting test, and the measurement may be combined with the process monitoring routines. The methodology presented can be, after slight adaptations, applied for material characterization during processing on other machines with different cutting kinematics, such as bandsaws, sash gang saws or routers.

Acknowledgments

Authors acknowledge Professor Tony Atkins of Reading University (UK) for valuable and inspirational advices.

Special thanks to ASPI TECH Sp. z o.o., Sp. k. (PL) for circular saw blades data, and Complex Sawmill in Dziemiany (Poland) for support and wood samples used in the experiments.

Part of this work has been conducted within the framework of the project SLOPE receiving funding from the European Union's Seventh Framework Programme for research, technological development and demonstration under the NMP.2013.3.0-2 (Grant number 604129), and project Bio4ever (RBSI14Y7Y4) funded within a call SIR (Scientific Independence of young Researchers) by MIUR.

Part of this work has been presented during Shatis 2015 (Wroclaw, Poland) and 22nd IWMS (Quebec, Canada) conferences.

We would like to thank anonymous reviewers for their constructive input and valuable suggestions.

References

[1] Agapov AI. Dinamika processa pilenija drevesiny na lesopiĺnych ramach. Dynamics of wood sawing on frame sawing machines. Goŕkij: Kirovskij Politechničeskij Institut, Izdanije GGU; 1983 [in Russian].
[2] Akonoa AT, Ulm FJ. An improved technique for characterizing the fracture toughness via scratch test experiments. Wear 2014;313(1–2):117–24. http://dx.doi.org/10.1016/j.wear.2014.02.015.
[3] Anderson TS. Fracture mechanics. CRC Press; 2005.
[4] Atkins AG. The science and engineering of cutting. The mechanics and process of separating, scratching and puncturing biomaterials, metals and non-metals. Oxford: Butterworth-Heinemann is an imprint of Elsevier; 2009.
[5] Atkins AG, Vincent JFV. An instrumented microtome for improved histological sections and the measurement of fracture toughness. J Mater Sci Lett 1984;3:310–21.
[6] Atkins AG. Modelling metal cutting using modern ductile fracture mechanics: quantitative explanations for some longstanding problems. Int J Mech Sci 2003;45:373–96. http://dx.doi.org/10.1016/S0020-7403(03)00040-7.
[7] Atkins AG. Toughness and cutting: a new way of simultaneously determining ductile fracture toughness and strength. Engng Fract Mech 2005;72(6):849–60. http://dx.doi.org/10.1016/j.engfracmech.2004.07.014.
[8] Aydin S, Yardimci MY, Ramyar K. Mechanical properties of four timber species commonly used in Turkey. Turkish J Eng Environ Sci 2007;31(1):19–27.
[9] Barnett AC, Lee YS, Moore JS. Fracture mechanics model of needle cutting tissue. J Manuf Sci Eng 2015;138(1):8p. http://dx.doi.org/10.1115/1.4030374.
[10] Beer P, Sinn G, Gindl M, Tschegg S. Work of fracture and of chips formation during linear cutting of particle-board. J Mater Process Technol 2005;159:224–8. http://dx.doi.org/10.1016/j.jmatprotec.2004.05.009.
[11] Blackman BRK, Hoult TR, Patel Y, Williams JG. Tool sharpness as a factor in machining tests to determine toughness. Eng Fract Mech 2013;101:47–58. http://dx.doi.org/10.1016/j.engfracmech.2012.09.020.
[12] Böllinghaus T, Byrne G, Cherpakov BI, Chlebus E, Cross CE, Denkena B, et al. Manufacturing engineering. In: Grote KH, Antonsson EK, editors. Springer handbook of mechanical engineering. Würzburg: Springer; 2009. p. 609–56. 10.1007/978-3-540-30738-9_7.
[13] Chuchała D, Orlowski KA, Sandak A, Sandak J, Pauliny D, Barański J. The effect of wood provenance and density on cutting forces while sawing Scots pine (*Pinus sylvestris* L.). BioRes 2014;9(3):5349–61. http://dx.doi.org/10.15376/biores.9.3.5349-5361.
[14] Csanády E, Magoss E. Mechanics of wood machining. Berlin, Heidelberg: Springer–Verlag; 2013. http://dx.doi.org/10.1007/978-3-642-29955-1. ISBN 978-3-642-29954-4.
[15] Ekevad M, Marklund B, Gren P. Wood-chip formation in circular saw blades studied by high-speed photography. Wood Mat Sci Eng 2012;7(3):115–9. http://dx.doi.org/10.1080/17480272.2011.629057.
[16] Franz NC. An analysis of the wood-cutting process. Ann Arbor: The University of Michigan Press; 1958.
[17] Gere JM. Mechanics of materials. Thomson Learning Inc.; 2004. <http://www.hljp.edu.cn/attachment/20120820084627006.pdf> [accessed on 29.07.2016].
[18] Glass SV, Zelinka SL. Moisture relations and physical properties of wood (Chapter 4). In: Wood Handbook – Wood as an Engineering Material (Centennial Edition). General Technical Report FPL-GTR-190. Madison, WI: U.S. Department of Agriculture, Forest Service, Forest Products Laboratory; 2010. 508 p. <http://www.fpl.fs.fed.us/documnts/fplgtr/fpl_gtr190.pdf> [accessed 29.04.2015].
[19] Green DW. Wood: Strength and stiffness. In: Encyclopedia of materials: science and technology. Encyclopedia of Materials: Science and Technology. Elsevier Science Ltd.; 2001. p. 9732–6. <https://www.fpl.fs.fed.us/documnts/pdf2001/green01d.pdf> [accessed 07.01.2017].
[20] Hellström LM, Biller SO, Edvardsson S, Gradin P. A theoretical and experimental study of the circular sawing process. Holzforschung 2013;68(3):307–12. http://dx.doi.org/10.1515/hf-2013-0066.
[21] Hlaskova L, Orlowski KA, Kopecký Z, Jedinák M. Sawing processes as a way of determining fracture toughness and shear yield stresses of wood. BioRes 2015;10(3):5381–94. http://dx.doi.org/10.15376/biores.10.3.5381-5394.
[22] Jockwer R, Steiger R, Frangi A. State-of-the-art review on approaches for the design of timber beams with notches. J Struct Eng 2013;140(3):04013068-1–04013068-13. http://dx.doi.org/10.1061/(ASCE)ST.1943-541X.0000838.
[23] Kivimaa E. Cutting force in woodworking. Helsinki: Julkaisu 18 Publication; 1950.
[24] Kopecký Z, Hlásková L, Orlowski K. An innovative approach to prediction energetic effects of wood cutting process with circular-saw blades. Wood Res 2014;59(5):827–34.
[25] Kretschmann DE. Chapter 5, mechanical properties of wood. In: Wood Handbook, Wood as an Engineering Material. General Technical Report FPL-GTR-190. Madison, WI: U.S. Department of Agriculture, Forest Service, Forest Products Laboratory. Centennial Edition; April 2010. 508 p.
[26] Kruzica JJ, Kim DK, Koester KJ, Ritchie RO. Indentation techniques for evaluating the fracture toughness of biomaterials and hard tissues. J Mech Behav Biomed Mater 2009;2:384–95. http://dx.doi.org/10.1016/j.jmbbm.2008.10.008.
[27] Krzosek S. Wytrzymałościowe sortowanie polskiej sosnowej tarcicy konstrukcyjnej różnymi metodami. In Polish: Strength grading of Polish structural sawn timber with different methods. Warszawa: Wydawnictwo SGGW; 2009.
[28] Laternser R, Gänser HP, Taenzer L, Hartmaier A. Chip formation in cellular materials. Transact ASME 2003;125:44–9. http://dx.doi.org/10.1115/1.1526126.
[29] Li H, Qin X, He G, Jin Y, Sun D, Price M. Investigation of chip formation and fracture toughness in orthogonal cutting of UD-CFRP. Int J Adv Manuf Technol 2016;82(5):1079–88. http://dx.doi.org/10.1007/s00170-015-7471-x.
[30] Liu J. Analysis of off-taxis tension test of wood specimens. Wood Fiber Sci 2002;34(2):205–11.

[31] McKenzie WM. Fundamental analysis of the wood-cutting process PhD thesis. MI, USA: University of Michigan; 1961.
[32] Merhar M, Bučar B. Cutting force variability as a consequence of exchangeable cleavage fracture and compressive breakdown of wood tissue. Wood Sci Technol 2012;46(5):965–77. http://dx.doi.org/10.1007/s00226-011-0457-4.
[33] Ohtani T, Iida R. Mechanical analysis of shear zone in chip formation process of wood cutting. In: Proc of 22nd international wood machining seminar, Hernandez R, Caceres C (editors), June 14–17, Quebec, Canada, Laval University, FPInnovations, Volume 1: oral presentations; 2015. p. 38–45.
[34] Orlicz T. Obróbka drewna narzędziami tnącymi. Wood processing with cutting tools. Warszawa: Skrypty SGGW-AR w Warszawie, Wydawnictwo SGGW-AR, Warszawa; 1998 [in Polish].
[35] Orlowski K. Experimental studies on specific cutting resistance while cutting with narrow-kerf saws. Adv Manuf Sci Technol 2007;31(1):49–63.
[36] Orlowski K, Ochrymiuk T, Atkins A, Chuchala D. Application of fracture mechanics for energetic effects predictions while wood sawing. Wood Sci Technol 2013;47:949–63. http://dx.doi.org/10.1007/s00226-013-0551-x.
[37] Orlowski K, Sandak J, Sandak A, Riggio M. Sposób wyznaczenia odporności na pękanie lub złamanie i sposób wyznaczenia wytrzymałości na ścinanie elementów wykonanych z materiałów ortotropowych, zwłaszcza z drewna. Patent pending: P406719; 2013.
[38] Orlowski KA, Atkins AG. Determination of the cutting power of the sawing process using both preliminary sawing data and modern fracture mechanics. In: Navi P, Guidoum A, editors. Proceedings of the third international symposium on wood machining. Fracture mechanics and micromechanics of wood and wood composites with regard to wood machining, 21–23 May, Lausanne, Switzerland. Presses Polytechniques et Universitaires Romandes, Lausanne; 2007. p. 171–4.
[39] Orlowski KA, Ochrymiuk T, Atkins AG. Specific cutting resistance while sawing of wood – the size effect. Ann WULS-SGGW, Forest Wood Technol 2010;72:03–107.
[40] Orlowski KA, Ochrymiuk T, Lackowski M. Empirical verification in industrial conditions of fracture mechanics models of cutting power prediction. Ann WULS, Forest Wood Technol 2014;85:162–7.
[41] Orlowski KA, Pałubicki B. Recent progress in research on the cutting process of wood. A review COST Action E35 2004–2008: wood machining—micromechanics and fracture. Holzforschung 2009;63:181–5. http://dx.doi.org/10.1515/HF.2009.015.
[42] Patel Y, Blackman BRK, Williams JG. Determining fracture toughness from cutting tests on polymers. Eng Fract Mech 2009;76(18):2711–30. http://dx.doi.org/10.1016/j.engfracmech.2009.07.019.
[43] Patel Y, Blackman BRK, Williams JG. Measuring fracture toughness from machining tests. Proc Inst Mech Eng Part C-J Eng Mech Eng Sci 2009;223 (12):2861–9. http://dx.doi.org/10.1243/09544062JMES1497.
[44] Prokofiev GF. Intensifikacija pilenija drevesiny ramnymi i lentočnymi pilami. Moskva: Lesnaja Promyslennost'; 1990 [in Russian].
[45] River HB, Vick CB, Gillespie RH. In: Minford DJ, editor. Wood as an adherend. (Chapter 1, from volume 7: Treatise on adhesion and adhesives). New York: Marcel Dekker Inc; 1991.
[46] Samarasinghe S, Kulasiri GD. Displacement fields of wood in tension based on image processing: Part 1. Silva Fennica 2000;34(3):251–9.
[47] Scholz F, Troeger J. Modelling of cutting forces. In: Proc of 17th international wood machining seminar, Yuri Stakhiev Seminar. In: Lachenmayr, G, Scholz F, editors. Rosenheim, Sept. 26–28. Germany, University of Applied Sciences, Retru-Verlag e.K., Weyarn, Part 2: Posters; 2005.
[48] Stanzl-Tschegg SE, Tan DM, Tschegg EK. New splitting test method for wood fracture characterization. Wood Sci Technol 1995;29:31–50. http://dx.doi.org/10.1007/BF00196930.
[49] Stanzl-Tschegg SE, Navi P. Fracture behaviour of wood and its composites. A review COST Action E35 2004–2008: wood machining – micromechanics and fracture. Holzforschung 2009;63(2):139–49. http://dx.doi.org/10.1515/HF.2009.012.
[50] Vasić S, Ceccotti A, Smith I, Sandak J. Deformation rates effects in softwoods: crack dynamics with lattice fracture modelling. Engng Fract Mech 2009;76(9):1231–46. http://dx.doi.org/10.1016/j.engfracmech.2009.01.019.
[51] Wang H, Chang L, Ye L, Williams JG. Micro-cutting tests: a new way to measure the fracture toughness and yield stress of polymeric nanocomposites. In: Proceedings of the 13th international conference on fracture, Beijing, China, June 16–21; 2013.
[52] Wang H, Chang L, Ye L, Williams JG. On the toughness measurement for ductile polymers by orthogonal cutting. Engng Fract Mech 2015;149:276–86. http://dx.doi.org/10.1016/j.engfracmech.2015.06.067.
[53] Williams JG, Patel Y, Blackman BRK. A fracture mechanics analysis of cutting and machining. Engng Fract Mech 2010;77:293–308. http://dx.doi.org/10.1016/j.engfracmech.2009.06.011.
[54] Wyeth DJ, Goli G, Atkins AG. Fracture toughness, chip types and the mechanics of cutting wood. A review COST Action E35 2004–2008: wood machining – micromechanics and fracture. Holzforschung 2009;63:168–80. http://dx.doi.org/10.1515/HF.2009.017.